Istraživanja i projektovanja za privredu
ISSN 1451-4117
DOI:10.5937/jaes0-54394
www.engineeringscience.rs

iipp publishing

Journal of Applied Engineering Science
Vol. 23, No. 1, 2025
Original Scientific Paper
Paper number: 23(2025)1, 1257, 112-120

EFFECT OF VOLUME-TO-EXPOSED-SURFACE RATIO ON TEMPERATURE AND MAXIMUM ALLOWABLE CASTING TEMPERATURE OF MASS CONCRETE

Adek Tasri*

Mechanical Engineering Department, Universitas Andalas, Indonesia
** adek.tasri@eng.unand.ac.id*

For mass concrete, it is well known that a high temperature or temperature differential at an early age can lead to cracks. The temperature and temperature differential are determined by several factors, such as the hydration heat, casting temperature, and mass concrete size. In this study, we numerically calculate the effects of mass concrete size, which is considered in the form of volume-to-exposed-surface ratio (V/A), on the temperature and temperature differential of the mass concrete at various casting temperatures. The data from the numerical calculation was then used to obtain the maximum allowable casting temperature as a function of concrete size. The hydration heat required for the numerical calculation was obtained using an adiabatic calorimeter. The study shows that there is a strong relationship between the maximum allowable casting temperature and the concrete dimension in the form of V/A. The Maximum allowable casting temperature versus concrete dimension curve obtain in this work is useful as a complement to the maximum casting temperature rules commonly used in current practical applications that do not consider the size of the concrete. Based on the concrete composition and environment temperature considered in this study, which is commonly used in practical applications in Indonesia, the maximum allowable casting temperature for V/A of 4,5; 3,0 and 1,5 m are found to be 22,2 ^{O}C, 27,1 ^{O}C,and 41,2 ^{O}C, respectively. The study also found that the difference in core and surface temperatures during early age did not cause a significant difference in strength at both locations.

Keywords: maximum casting temperature, temperature differential, mass concrete temperature, hydration heat

1 INTRODUCTION

It is well known that most of the heat generated during cement and water hydration is confined to the core region of mass concrete because of the low thermal conductivity of concrete. While in the surface region, heat is released into the environment via convection. Thus, the core has a higher temperature than that of the surface, cracks could develop in the mass concrete [1, 2]. If the mass concrete temperature is too high, exceeding 70 ^{O}C [3] the ettringite that forms at the beginning of hydration decomposes into monosulphate ions and sulphate, as reported by Taylor et al. [4]. After several months, monosulphate ions and sulphates react again to form ettringite. This process is known as delayed ettringite formation (DEF). Because the volume of ettringite formed in this second round is larger than the volume of the reactants, cracks can develop inside the mass concrete. Furthermore, when the hydration process involves high temperatures, it can lead to faster initial strength development and lower strength in the later stages, finally lowering the structure's durability as a whole. Therefore, mass concrete temperature must be controlled to avoid cracks and increase durability.

Considering the importance of temperature control of mass concrete, several efforts have been made to realize it. A commonly used method for temperature control is post-cooling, wherein cool water is passed through pipes embedded in mass concrete to cool down the concrete during the hydration period. Post-cooling has gained considerable popularity in controlling mass concrete temperature as it was first used at the Owyhee Dam in Oregon in 1931 [5]. However, post-cooling is relatively expensive and can result it cracks around the cooling pipe if the water temperature is too low compared with the mass concrete temperature [6, 7]. Another effort to control the temperature of mass concrete is to reduce the amount of heat generated during the hydration reaction by substituting cement with pozzolanic materials, such as fly ash and silica fume [8, 9, 10]. ACI 207 [11] recommends reducing the concrete temperature by reducing the casting temperature, which can be achieved by cooling down concrete-forming components.

In several European countries, a practical approach was made to ensure that cracks do not occur by limiting the temperature differential, the difference between core and surface temperature, in concrete at most 20 ^{O}C [13] so the strain or stress does not exceed the concrete's ultimate strain or strength. Gajda and Vangeem [13] found that for a concrete block with a temperature differential of 20 ^{O}C, the maximum compressive stress caused by internal and external strain is less than 1000 Psi. Due to most mass concrete having a compressive strength of more than 1000 Psi, a temperature differential limit of 20 ^{O}C is very safe.

In order to keep the temperature differential from exceeding 20 ^{O}C limit, the amount of heat trapped in the core of the concrete block needs to be reduced; this can be achieved several ways, one of them is by reducing the casting temperature, as a lower casting temperature can decrease the hydration heat evolution rate [12, 14,15]. Although a lower casting temperature will reduce early-age compressive strength, it increases seven-day compressive strength [16, 17]. ACI 207 [11], ACI 301.5 [18], and ASTM C94 [19] also recommend reducing casting temperature but have

not imposed any limit. Temperature restrictions are available in ASTM C 1064-86 [20], wherein the casting temperature is limited to 35 ^{O}C. Australian standard AS 1379 [21] requires the casting temperatures to be in the 5–35 ^{O}C range in hot weather conditions. Nasir et al. [22] suggested that the optimum casting temperatures for plain and blended cement concrete were 32 ^{O}C and 38 ^{O}C, respectively.

So far, the casting temperature limitations avoid the effect of concrete size. Although, the increase in size causes an increase in the amount of heat trapped inside the concrete so that the temperature differential could rise beyond the 20 ^{O}C limit.

In this study, we numerically calculate the casting temperature limit by considering the concrete size. For the results to apply to many concrete shapes, size is regarded as a volume-to-exposed-surface ratio (V/A). The results of this study are expected to be useful in determining the casting temperature as a function of concrete size in practical applications. We also studied the effects of casting temperature and concrete size on the strength of core and surface of concrete, during the early age. The hydration heat data required for the numerical simulation were measured using a diabatic calorimeter.

2 *MATERIALS AND MEHODS*

The determining the maximum allowable casting temperature is started by measuring the change in concrete temperature during the hydration process using an adiabatic calory meter. The temperature data is then used to obtain the hydration heat rate, which is used in a numerical simulation to get the maximum temperature differential as a function of the casting temperature at several V/A. The next step is to identify the casting temperature that produces a maximum differential temperature of 20 ^{0}C. This casting temperature is the maximum allowed casting temperature.

2.1 Hydration Heat Measurement

The concrete we studied is commonly used as a foundation for practical applications in Indonesia. It is expected to have a strength of 31.6 MPa. Based on the Indonesian standard for concrete, SNI 03-2834-2002, the composition of the concrete components used to obtain this strength was 0.192, 0.286, 0.092, and 0.430 kg of cement, sand, water, and gravel per kg of concrete, respectively.

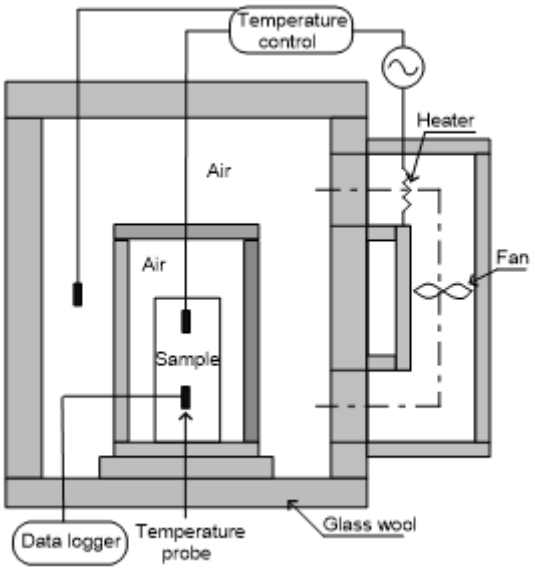

Fig. 1. Schematic arrangement of adiabatic calorimeter

The adiabatic calorimeter used in this study to determine the hydration heat was similar to that used by Ballim and Graham [23]. A schematic of the calorimeter is shown in Fig. 1. One kilogram of sample, with an initial temperature 35 ^{O}C, was placed in a container in a tank. During the hydration, the sample temperature and the air temperature around the sample were kept the same to prevent heat loss from the sample to the surroundings. This was achieved using a temperature controller that turns on the heater if the air temperature around the sample is lower than the sample temperature. The sample temperature was recorded every 30 min using a data logger.

2.2 Numerical Calculation Model

Applying the energy conservation principle to a volume of mass concrete at an early age, where the hydration heat produced during a time *dt* is equal to the increasing internal energy plus heat transferred to the surroundings, yields

$$\dot{q}Vdt = \rho VC_P dT + Ah(T - T_a)dt \quad (1)$$

Replace $dT$with $d(T - T_a)$, result

$$\frac{d(T-T_a)}{(T-T_a)} = (\frac{\dot{q}}{\rho C} - \frac{Ah}{\rho VC})dt \quad (2)$$

where $\dot{q}$, ρ,C, h and V are the hydration heat rate in (J/sm^3), density, specific heat, and convective heat-transfer coefficient and concrete volume, respectively; and T and T_a are the concrete average temperature, and ambient air temperature. Eq. (1) and (2) show that the volume-to-exposed surface ratio (*V/A*) is one of the parameters that determine the concrete temperature at left hand side of Eq. (2). Using *V/A* as a concrete temperature parameter is also found in ACI 207 [11], Do et al. [24] and Li et al. [25].

In this study, numerical simulations were performed to calculate concrete temperature for several variations in the *V/A* and casting temperature using the commercial software ANSYS 2022R1. The governing equation for numerical simulations is the heat conduction equation, which is known as the Fourier-Biot equation. It can be expressed as:

$$\rho C_P \frac{\partial T}{\partial t} = \nabla \cdot k\nabla T + \dot{q} \quad (3)$$

with *k* is thermal conductivity. *k* and other concrete thermal properties presented in Table 1. Considering the effect of time and temperature history on $\dot{q}$, as recommended by Ballim [23], $\dot{q}$was determined using a chain rule as the maturity heat rate multiplied by the rate of maturity change, as presented in Eq. (4):

$$\dot{q} = \frac{\partial q}{\partial m}\frac{\partial m}{\partial t} \quad (4)$$

m indicates the maturity, which can be expressed as the equivalent maturity of the concrete cured at 20 ^{O}C using the Arrhenius maturity function [23]:

$$m = \sum_{i=1}^{n} exp\left(\frac{E}{R}(\frac{1}{273} - \frac{1}{T_i}\right)(t_i - t_{i-1}) \quad (5)$$

where E = 33kJ/h and R = 8.31 J/h denote the concrete activation energy and universal gas constant;$T_i$represents the average temperature during interval $(t_i - t_{i-1})$. $q$in Eq.(4) is the cumulative hydration heat in (*J/m³*), which was calculated as the product of$\rho$and$C$ with the concrete temperature rise during the adiabatic hydration reaction.

$$q = \rho C_p(T_t - T_s) \quad (6)$$

where T_t is the temperature of mass concrete at time t and T_s is the initial temperature. Herein, T_t was obtained from adiabatic calorimeter measurements. The volumetric hydration heat $\dot{q}$ in Eq. (4) is then written in C^{++} code and attached to ANSYS as a user-defined function (UDF).

Following the discretization procedure of the finite volume algorithm, the governing equation, Eq. (3), is integrated over a control volume *P* that have a volume of $\Delta\Omega$ and over a time interval form t to $t + \Delta t$gives.

$$\int_{\Delta t}\int_{\Delta\Omega} \rho C \frac{\partial T}{\partial t}\, d\Omega dt + \int_{\Delta t}\int_{\Delta\Omega} \nabla \cdot k\nabla T\, d\Omega dt = \int_{\Delta t}\int_{\Delta\Omega} \dot{q}\, d\Omega dt \quad (7)$$

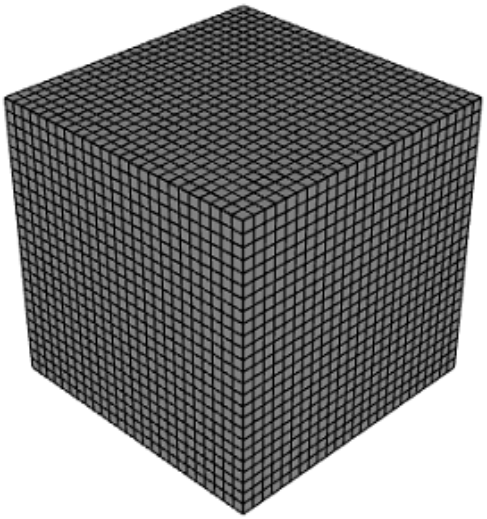

Fig. 2. The mass concrete calculation domain and hexahedral finite volume mesh

Applying the divergence theorem to Eq. (7) yields

$$\int_{\Delta\Omega}((\rho CT)^1 - (\rho CT)^0)\, d\Omega + \int_{\Delta t}\int_A k\nabla T \cdot d\vec{A}dt = \int_{\Delta t}\int_{\Delta\Omega} \dot{q}\, d\Omega dt \quad (8)$$

The superscripts 1 and 0 in the first term of Eq. (8) denote the values at the times$t + \Delta t$and$t$, respectively. For stability and simplification reasons, the implicit integral scheme was applied to solve Eq. (8) on the control volume P, results

$$((\rho C_P T_P)^1 - (\rho C_P T_P)^0)\Delta\Omega + \sum_{f=1}^{nb}\left(k\nabla T_f^1 \cdot \vec{A}_f \Delta t\right) = \dot{q}_P \Delta\Omega\Delta t \quad (9)$$

Subscibe *P* and *f* in Eq. (9) represent centre and surfaces centre of control volume *P*. Therefore, we can rearrange Eq. (9) to give a discretised form of governing equation on a control volume *P* as shown in Eq. (10). Eq. (10), then solve for the temperature at the finite-volume cell centre, T_p.

$$\frac{\Delta\Omega\rho C T_P^1}{\Delta t} = \frac{\Delta\Omega\rho C T_P^0}{\Delta t} + \sum_{f=1}^{nb}\left(k\nabla T_f^1 \cdot \vec{A}_f\right) + \dot{q}_P\Delta\Omega \quad (10)$$

The mass concrete was modelled as a cube. The calculation domain and hexahedral mesh used for simulation are illustrated in Fig. 2. The concrete has horizontal surfaces of 3 m × 3 m, with a height determined from the *V/A*. *V/A* values of 0.75, 1, 1.5, 1.75 and 2 m were used in this study.

Numerical simulations were performed at several casting temperatures: 20 ^{O}C, 25 ^{O}C, 27.5 ^{O}C, 30 ^{O}C and 35 ^{O}C. The maximum temperature of 35 ^{O}C is based on the limits recommended by AS 1379 [21].

The vertical surfaces of the concrete were defined as adiabatic boundaries. The heat leaves the concrete block through the top and bottom surfaces by convection. The expression for convective heat transfer coefficient for the convective boundary was obtained from a textbook by Changel [26]. It is given as follows:

$$h = 9.60 + 1.12U \quad (11)$$

Where *U* is the average wind speed in Indonesia which is 2.0 m/s.

Table 1. Concrete thermal properties

Properties	
Thermal conductivity [J/(s m ^{0}C)]	2.5
Spesific heat [J/(kg ^{0}C)]	1400
Density [kg/m^3]	2420

3 RESULT AND DISCUSTION

The temperatures during the hydration process are shown in Fig. 3. Temperature changes during the initial hydrolysis were not visible in the figure as the process occurred very quickly, and the heat released was less compared to the total heat released during the hydration reaction. The temperature started to rise at the end of the dormant period and reached its highest value of 65.0 ^{O}C. The temperature data were used to calculate the cumulative hydration heat, required in numerical calculation using Eq. (6).

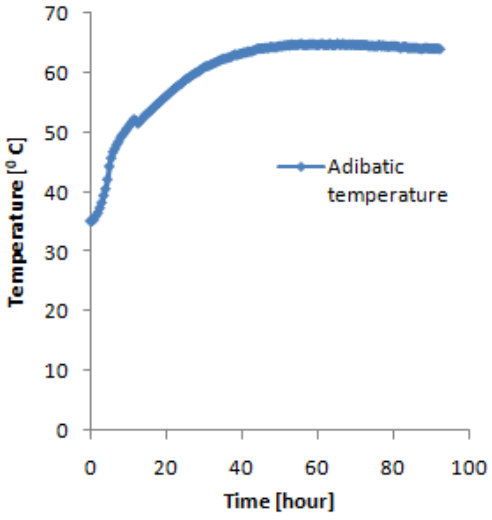

Fig. 3. Concrete temperature rise measured using adiabatic calorimeter

In steady-state conditions, the core temperature is directly proportional to hydration heat as indicated by the solution of the Fourier-Biot equation (Eq. (3)) under steady-state conditions and constant heat source at a particular time t as shown in Eq. (12).

$$T_C - T_a = 0.125\frac{\dot{q}L^2}{k} + \frac{1}{2}\frac{\dot{q}L}{h} \quad (12)$$

h, T_C, T_a in Eq. 12 are convective heat transfer coefficient, core and ambient air temperature, respectively. *L* is the concrete block's height, equal to (2 *V/A)*. In actual unsteady conditions, the core temperature is higher than in a steady state due to some heat trapped in the concrete core. The increase in temperature causes an increase in the hydration rate, which leads to a much higher core temperature, as reported by Escalante-Garcıa and Sharp [27] and Lot henbach et al. [28]. Eq. 12 shows that the core temperature increase by increasing in L or V/A.

Core temperatures at various V/A are shown in Fig. 4. For L=4m or V/A=2m, the maximum temperature is 67C. This temperature was determined using adiabatic conditions for vertical walls. In practical application, the core temperature can be slightly lower than 67 ^{0}C because the assumption of the adiabatic condition for the vertical wall in numerical calculation is not completely meet the real situation. Thus, the core temperature is still below the DEF temperature of 70 ^{0}C, which does not lead to an expansive reaction subsequent crack caused by ettringite formations.

This data is helpful in practical applications where at V/A less than 2m, the maximum temperature of concrete (with materials and environmental conditions similar to the model used in this study) is less than 70 ^{0}C, so cracks caused by DEF do not occur. However, If V/A is more than 2m, the maximum temperature can exceed 70 ^{0}C, and cracks can occur due to the DEF process. At high temperature cracks can also occur due to expansion and shrinkage that are blocked by friction between the concrete and its base or water evaporating from the concrete, which can lead to shrinkage and microcracks. In this condition, prevention needs to be done through a precooling process by lowering the temperature of the concrete-forming components such as water, cement and gravel before being mixed to form concrete or using a post-cooling system where cooling water flows through a network of pipes planted in the concrete.

Although V/A significantly affects core temperature, this is not true for surface temperature, where V/A does not seem to have much effect on surface temperature due to convection heat release from the surface to the surroundings. The increase in core temperature that is not followed by surface temperature causes shrinkage and deformation of the concrete surface; under internal constraints, temperature cracks easily occur.

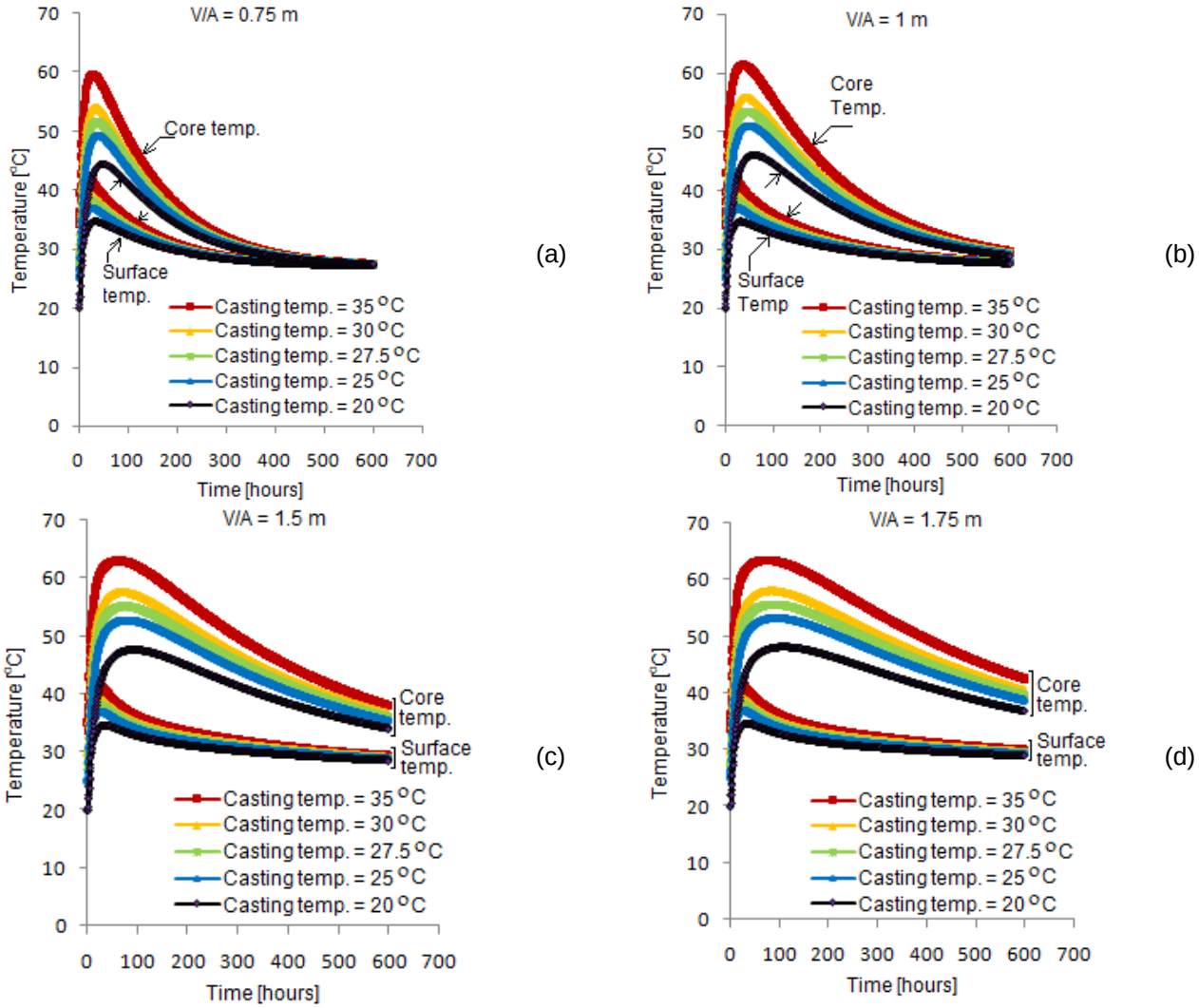

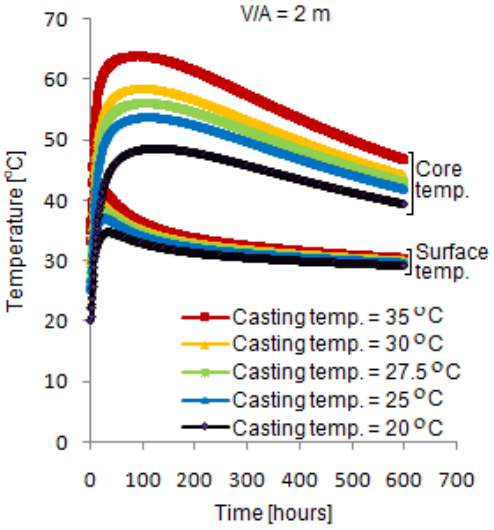

(e)

Fig. 4. Temperature variation over time (a) V/A = 0,75 m; (b) V/A = 1m; (c) V/A = 1,5 m; (d) V/A = 1,75 m; (e) V/A = 2m

The maximum core and surface temperature differential of the concrete is known as maximum temperature differential and denote byΔT_{max} is plotted in Fig. 5. Fig. 5a shows that ΔT_{max} was strongly influenced by *V/A*. At a specific value of *V/A*, ΔT_{max} increased linearly with the casting temperature. To keep ΔT_{max} from exceeding 20 ^{O}C where cracking begins to occur, the casting temperature must be limited. The differential temperature limit of 20 ^{O}C is used as a reference [13] because the thermal stress that occurs at that temperature (around 1000 Mpa) is far below the strength of most concrete structures in practical applications, so this limit is considered safe for all concrete conditions. However, in some cases, this limit is very conservative; for certain concretes, it can be greater than 20 ^{O}C.

Applying the limit ΔT_{max}= 20 C, from Fig. 5a, it can be observed that for V/A of 0,75 m, 1 m, 1,5 m, 1,75 m and 2,0 m, the maximum allowable casting temperatures are 37,5 ^{O}C, 32,2 ^{O}C, 27,2 ^{O}C, 25,5 ^{O}C and 24,3 ^{O}C, respectively. The data is presented graphically in Fig. 5b. This data provides convenience in practical applications because the maximum allowable casting temperature can vary depending on the size of the concrete, not necessarily at a specific value as in current concrete work regulations.

For high strength concrete, ΔT_{max} may be more than 20 ^{O}C, so the maximum allowable casting temperature can be determined from Fig. 5a using the abovementioned procedure. However, increasing the ΔT_{max} limit above 20 ^{0}C needs to be done carefully so that the stress that occurs does not exceed the strength of the concrete during the hydration process at an early age. The calculation will be quite complicated and requires data on the compressive strength of concrete that changes according to the maturity level of the concrete. The use of data in Fig. 5 will avoid these complicated calculations. These data are useful as a quick guidance for determining the casting temperature of concrete using materials and compositions similar to those used in this study, such as those widely used in Indonesia, without the need to do laboratory work to measure hydration heat and perform complex calculations.

Fig. 5b also shows that the maximum allowable casting temperatures nonlinearly increase with a decrease in *V/A*. Although for low *V/A* the allowable casting temperature can be high, it should not be too high as the high temperature can cause a non-uniform distribution of hydration products, which makes the concrete has high porosity and lower long term compressive strength [29,30].

The differences in core and surface temperatures cause differences in maturity in the two locations, as presented in Fig. 6. Referring to Fig. 6d, at *V/A*= 2 m, the surface and core maturity 600 hours after initiating hydration is 1200 hours and 2700 hours, respectively. Using Hansen and Pedersen's [31] strength equation, Eq. (13), it can be revealed that the difference in core and surface strength is only about 1%.

$$S = S_U e^{-(\frac{\tau}{M})\alpha} \quad (13)$$

S_u, τ and α are constants that have the value of 4583 Psi, 57 and 0.56 respectively. This result indicates that difference in core temperature and the surface temperature does not cause a significant difference in the strength of the concrete at the two locations.

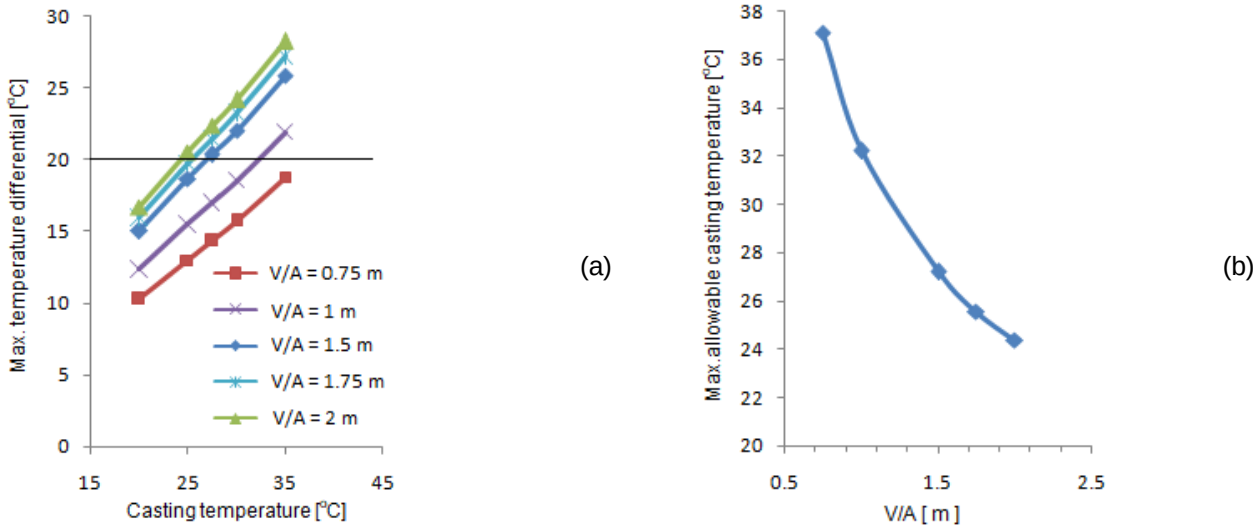

Fig. 5. (a) Maximum temperature-differential with respect to casting temperature and (b) maximum allowable casting temperature with respect to and *V/A*

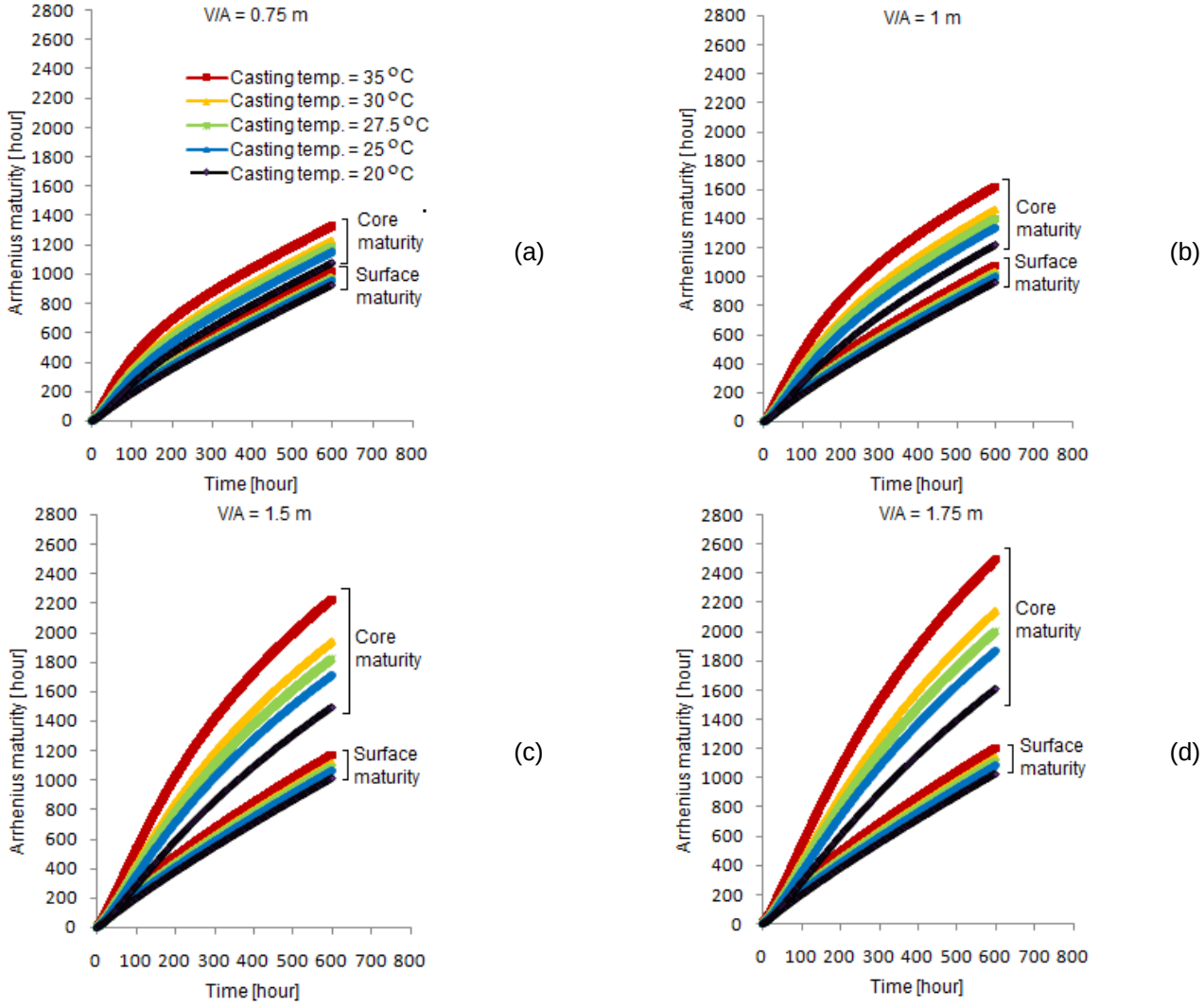

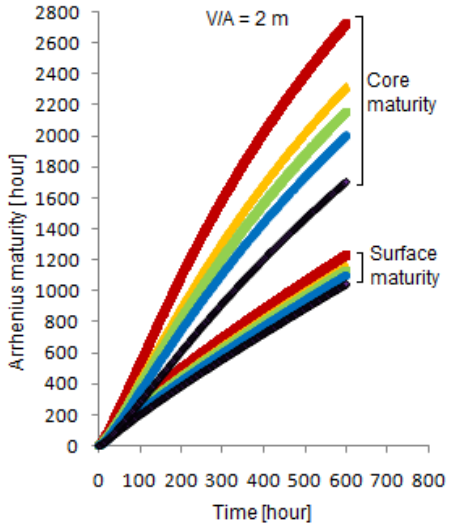

(e)

Fig. 6. Arrhenius maturity of core and surface. (a) V/A = 0,75 m; (b) V/A = 1m; (c) V/A= 1,5m; (d) V/A = 1,75 m; (e) V/A = 2m; Chart legends are found in Fig. 6a

4 CONCLUSIONS

Experiments and numerical simulations were conducted to study the effect of volume-to- exposed surface ratio on temperature and maximum allowable casting temperature. The following data and conclusions were obtained.

1. Through hydration heat measurement and numerical simulation, it is found that there is a strong relationship between the maximum allowable casting temperature and the concrete dimension in the form of volume-to-exposed-surface ratio (V/A). This data provides convenience in practical applications because the maximum allowable casting temperature can vary depending on the size of the concrete, not necessarily at a specific value as in current concrete work regulations.
2. Based on concrete and environment data used in this study, which is commonly used in practical applications in Indonesia, the maximum allowable casting temperature for volume-to-exposed-surface ratio of 0,75 m, 1 m, 1,5 m, 1,75 m and 2 m are 37,5 ^{O}C, 32,2 ^{O}C, 27,2 ^{O}C, 25,5 ^{O}C and 24,3 ^{O}C, respectively.
3. An increase in volume-to-exposed-surface ratio or casting temperature increases the core temperature but does not affect the surface temperature of the mass concrete.
4. The difference in core and surface temperatures did not cause a significant difference in strength at both locations

5 ACKNOWLEDGMENT

The author would like to thank Mechanical Engineering Department, Universitas Andalas, Indonesia for full support for this research.

6 REFERENCES

[1] American Concrete Institute. (2005). Cooling and insulating system for mass concrete (ACI 207.4R-05). 207. ACI Committee.

[2] Portland Cement Asc. (2003). Design and Control of Concrete Admixtures 14th Edition–CD Version, CD100.1. Portland Cement Association.

[3] Department of Transportation (2009). Developmental Specifications for Mass Concrete -Control of Heat of Hydration. D.O.T.

[4] Taylor, H.F.W, Famy, C, Scrivener, K.L. (2001). Delayed ettringite formation. Cem. Concr. Res., vol. 31, no.5, pp.683-693. doi: 10.1016/S0008-8846(01)00466-5.

[5] Zuo, Z., Hu, Y., Li,Q., Zhang, L. (2014). Data mining of the thermal performance of cool-pipes in massive concrete via in situ monitoring. Math. Probl. Eng., Article ID 985659. doi: 10.1155/2014/985659.

[6] Tasri, A., Susilawati, A. (2019). Effect of cooling water temperature and space between cooling pipes of post-cooling system on temperature and thermal stress in mass concrete. Journal of Building Engineering, vol. 24, article ID 100731. doi: 10.1016/j.jobe.2019.100731.

[7] Tasri, A., Susilawati, A. (219). Effect of material of post-cooling pipes on temperature and thermal stress in mass concrete. Structures, vol. 20, pp.204-2014. doi: 10.1016/j.istruc.2019.03.015

[8] Ganjigatti,M., Kashinath,B.R., Prakash, K.B. (2015). Effect of Replacement of Cement by Different Pozzolanic Materials on Heat of Hydration and Setting Time of Concrete. Int. J. Environ. Agric. Res. IJOEA, vol.1, pp. 24-29.

[9] Sánchez de Rojas,M.I., Luxan,M.P., Frıas, M., Garcıa,N. (1993). The influence of different additions on Portland cement hydration heat. Cem. Concr. Res.vol. 1, pp. 46-54. doi: 10.1016/0008-8846(93)90134-U

[10] Frıas,M., Sánchez de Rojas,M.I., Cabrera, J. (2000). The effect that the pozzolanic reaction of metakaolin has on the heat evolution in metakaolin-cement mortars. Cem. Concr. Res., vol. 30, pp. 209-216. doi: 10.1016/S0008-8846(99)00231-8.

[11] American Concrete Institute, “Cooling and insulating system for mass concrete (ACI 207.4R-05)”, ACI Committee 207, 2005.

[12] Wang, j., Yan, P. (2006). Influence of initial casting temperature and dosage of fly ash on hydration heat evolution of concrete under adiabatic condition. Journal of thermal analysis and calorimetry, vol. 3, pp. 755-760. doi:10.1007/s10973-005-7141-6.

[13] Gajda, J., Vangeem, M. (2002). Controlling temperatures in mass concrete. Concrete international”, vol 24, pp.58-62.

[14] Kiernożycki,W., Błyszko, J. (2021). The Influence of Temperature on the Hydration Rate of Cements Based on Calorimetric Measurements”, Materials, vol. 14, pp. 3025. doi: 10.3390/ma14113025.

[15] Zhang, P., Xiong, H., Wang, R. (2022). Measurements and numerical simulations for cast temperature field and early-age thermal stress in zero blocks of high-strength concrete box girders. Advances in Mechanical Engineering, vol. 14, pp. 1-14. doi: 10.1177/16878132221091514.

[16] Wang, P.M., Liu, X.P. (2011). Effect of temperature on the hydration process and strength development in blends of Portland cement and activated coal gangue or fly ash. Journal of Zhejiang University-SCIENCE A, vol. 12, pp. 162-170. doi: 10.1631/jzus.A1000385.

[17] Burg, R.G. (1996) The influence of casting and curing temperature on the properties of fresh and hardened concrete, Portland Cement Association.

[18] American concrete institute, (2007). Cooling and insulating system for mass concrete (ACI 301.5), ACI Committee 207.

[19] American Society for Testing and Materials. (2009). Standard Specification For Ready-Mixed Concrete (ASTM C94M -09), American Society for Testing and Materials.

[20] American Society for Testing and Materials. (1986). Temperature of Freshly Mixed Hydraulic Cement Concrete (ASTM C1064-86), American Society for Testing and Materials.

[21] Australian Standard. (1997). Specification and supply of concrete (AS 1379), Australian Standard.

[22] Nasir,M, Al-Amoudi,O.S., Al-Gahtani, H.J., Maslehuddin, M. (2016). Effect of casting temperature on strength and density of plain and blended cement concretes prepared and cured under hot weather conditions. Construction and Building Materials, vol. 112, pp. 529-537. doi: 10.1016/j.conbuildmat.2016.02.211

[23] Ballim, Y., Graham, P.C. (2003). A maturity approach to the rate of heat evolution in concrete. Magazine of Concrete Research, vol. 3, pp. 249-156. doi: 10.1680/macr.2003.55.3.249.

[24] Do, T.A., Verdugo, D., Tia, M., Huang, T.T. (2021). Effect of volume-to-surface area ratio and heat of hydration on early-age thermal behavior of precast concrete segmental box girders. Case Stud. Therm. Eng, vol. 20, pp. 101448. doi: 10.1016/j.csite.2021.101448.

[25] Li, X., Zhu, H., Fu, Z., Liu, P., Xia, C. (2022). Influence of Volume-to-Surface Area Ratio on the Creep Behavior of Steel Fiber Ceramsite Concrete Beams. Coatings, vol. 12. Pp. 977. doi: 10.3390/coatings12070977

[26] Chengel, Y. (2002). Heat transfer: A practical approach, McGraw Hill.

[27] Escalante-Garcı´a, J.I., Sharp, H.J. (1998). Effect of temperature on the hydration of the main clinker phases in Portland cements: Part I, neat cements. Cem. Concr. Res., vol. 9, pp. 1245-1257. doi: 10.1016/S0008-8846(98)00115-X

[28] Lothenbach, B., Winnefeld, F., Alder, C., Wieland, E., Lunk, P. (2007). Effect of temperature on the pore solution, microstructure and hydration products of Portland cement pastes. Cem. Concr., vol. 37, pp. 483-497. doi: 10.1016/j.cemconres.2006.11.016.

[29] Kaleta-Jurowska, A., Jurowski, K. (2020). The influence of ambient temperature on high performance concrete properties. Materials, vol. 13, pp. 4646. doi: 10.3390/ma13204646.

[30] Khan, M.U., Nasir, M., Al-Amoudi,O.S.B., Maslehuddin, M. (2021). Influence of in-situ casting temperature and curing regime on the properties of blended cement concretes under hot climatic conditions. Construction and Building Materials, vol. 272, pp. 121865. doi:. 10.1016/j.conbuildmat.2020.121865

[31] Hansen, P.F., Pedersen, E.J (1985). Curing of Concrete Structures, Draft DEB-Guide to Durable Concrete Structures, Appendix 1, Comité EuroInternational du Béton, Switzerland.

Paper submitted: 26.10.2024.

Paper accepted: 27.02.2025.